Mon. Not. R. Astron. Soc. **000**, 1–9 (2017) Printed 11 January 2017 (MN LATEX style file v2.2)

Smoothing the Redshift Distributions of Random Samples for the Baryon Acoustic Oscillations : Applications to the SDSS-III BOSS DR12 and QPM Mock Samples

arXiv:1701.02427v1 [astro-ph.CO] 10 Jan 2017

Shao-Jiang Wang,[1,3,5⋆] Qi Guo,[2,4] Rong-Gen Cai,[1,3,5]

[1] *CAS Key Laboratory of Theoretical Physics, Institute of Theoretical Physics, Chinese Academy of Sciences, No.55 Zhong Guan Cun East Street, Beijing 100190, P.R. China*
[2] *National Astronomical Observatories, Chinese Academy of Sciences, 20A Datun Road, Chaoyang, Beijing 10012, P.R. China*
[3] *School of Physical Sciences, University of Chinese Academy of Sciences, No.19A Yuquan Road, Beijing 100049, P.R. China*
[4] *School of Astronomy and Space Science, University of Chinese Academy of Sciences, No.19A Yuquan Road, Beijing 100049, P.R. China*
[5] *Center for Gravitational Physics, Yukawa Institute for Theoretical Physics, Kyoto University, Kyoto 606-8502, Japan*

Accepted XXX. Received YYY; in original form ZZZ

ABSTRACT

We investigate the impact of different redshift distributions of random samples on the Baryon Acoustic Oscillations (BAO) measurements of $D_V(z)r_{\rm d}^{\rm fid}/r_{\rm d}$ from the two-point correlation functions (2PCF) of galaxies in the Data Release 12 (DR12) of the Baryon Oscillation Spectroscopic Survey (BOSS). Big surveys, such as BOSS, usually assign redshifts to the random samples by randomly drawing values from the measured redshift distributions of the data, which would necessarily introduce fiducial signals of fluctuations into the random samples, weakening the signals of BAO, if the cosmic variance cannot be ignored. We propose a smooth function of redshift distribution which fits the data well to populate the random galaxy samples. The resulting cosmological parameters match the input parameters of the mock catalogue very well. The significance of BAO signals has been improved by 0.29σ for low-redshift (LOWZ) sample and by 0.15σ for constant-stellar-mass (CMASS) sample, though the absolute values do not change significantly. Given the precision of the measurements of current cosmological parameters, it would be appreciated for the future improvements on the measurements of galaxy clustering.

Key words: galaxy survey, correlation function, random catalogues

1 INTRODUCTION

The Baryon Acoustic Oscillations (BAO) is an important tool in modern cosmology. It is the relic imprint of the matter perturbations when the sound waves stop propagating in the baryon-photon fluid after the recombination of the Universe. It is also a well-understood linear-theory phenomenon which usually serves as the standard ruler for the large-scale measurements of our Universe. When combined with other cosmological measurements, such as the SNIa, gravitational lensing, Cosmic Microwave Background (CMB) etc, it allows to explore the expansion history of the whole Universe and to constrain the cosmological parameters to a high precise level.

The measurements of BAO have made a great progress over the last decade. From the seminar works of the Two Degree Field Galaxy Redshift Survey (2dFGRS Cole et al. 2005) and the Sloan Digital Sky Survey (SDSS Eisenstein et al. 2005), followed by enlarged measurements of the WiggleZ survey (Blake et al. 2011a) and the Six Degree Field Galaxy Survey (6dFGRS Beutler et al. 2011), the measurements of BAO finally reached the milestone of 1 percent precision in SDSS-III Baryon Oscillation Spectroscopic Survey (BOSS) Data Release Eleven (DR11 Anderson et al. 2014b), which was consistent with the results of recent DR12 (Alam et al. 2015) of SDSS-III BOSS. In the final data release (Alam et al. 2016) of SDSS-III BOSS, the measure-

⋆ E-mail: schwang@itp.ac.cn

ments of BAO were carried out using a combined sample consisting of the CMASS, LOWZ, LOWZ2 and LOWZ3.

Anisotropy features have been found in BAO signals along radial and transverse directions, which arise from two main effects as follows. One is from the late-time non-linear evolutions of galaxy clustering. Eisenstein et al. (2007b); Padmanabhan et al. (2012) proposed to reconstruct the linear power spectrum to improve the BAO signals. The other is from both the redshift-space distortions (RSD) (Kaiser 1987) and the mismatched fiducial cosmology, namely the Alcock-Paczynski effect (Alcock & Paczynski 1979). The degeneracy between the Hubble parameter $H(z)$ and the angular diameter distance $D_A(z)$ can be broken by projecting galaxy clustering correlation along radial/transverse directions (Okumura et al. 2008; Gaztanaga et al. 2009; Blake et al. 2011b; Chuang & Wang 2012), or monopole/quadrupole moments (Padmanabhan & White 2008; Taruya et al. 2011; Chuang & Wang 2013; Xu et al. 2013) or the newly proposed wedge method (Kazin et al. 2012, 2013). More detailed discussions on the systematics of BAO can be found in Vargas-Magaña et al. (2016).

The two point correlation function (2PCF) of galaxies is one of the most popular method to estimate the BAO signals. It measures the pairwise excesses of the data galaxies in comparison with otherwise randomly distributed galaxies. The redshift distribution $N(z)$ for the random galaxy catalogues is supposed to be smooth, given the relatively slow evolution of the tracer galaxies. However, if the volume is small, the structures along line-of-sight direction usually manifest themselves as violent fluctuations in $N(z)$. If one assumes the redshift distributions of random samples to be the same as the data samples, it would bias the resulting clustering measurements. In the literatures, many works adopted a smoothed fitting function to describe the underlying $N(z)$. Shaun Cole (Cole 2011) developed a new algorithm to generate the random catalogue from the data catalogue consist of a simple flux-limited sample. It automatically provides the distribution of an unbiased $N(z)$ without assuming a prior fitting formula. For large galaxy survey, the volume is usually big enough so that the cosmic variance could be minor. In this case, redshifts of random galaxies are usually generated by randomly drawing from the measured galaxy redshifts with some weights (e.g. see Reid et al. 2016, section 5.2). Whether a random catalogue generated in this way could inherit fluctuations of the clustering signals and lead to a weakened BAO signal depends on the volume of the survey. Ross et al. (2012) demonstrated the systematic difference of spherically averaged correlation functions calculated with this redshift assignment scheme and that with "spline" approaches are negligible. However, their typical spline method adopted $\Delta z = 0.01$ to construct the random catalogue corresponding to $80 \sim 90\,\mathrm{Mpc}$, which is smaller than the typical scale of BAO, suggesting the random catalogue generated using this spline approach could also inherit the BAO signals along the redshift direction.

In this paper, we propose to use a new smoothed redshift distribution function for the random galaxy samples. We describe the data and mock catalogues in subsection 2.1, review the correlation function in subsection 2.2 and the fitting template in subsection 2.3. In section 3 we describe how we generate the random catalogues with a wiggly redshift distribution in subsection 3.1 and with a smoothed redshift distribution in subsection 3.2. The method validation is given in subsection 3.3 using QPM mock catalogues (White et al. 2014). In section 4 we apply the smooth method to the DR12 data catalogues and compare with results using wiggly method. The section 5 is the conclusions.

The fiducial cosmology we used in the paper is the same as those used in the SDSS-III BOSS DR12 (e.g. Cuesta et al. 2016): $h = 0.70$, $\Omega_\mathrm{m} = 0.29$, $\Omega_\Lambda = 0.71$, $\Omega_\mathrm{b}h^2 = 0.02247$, $n_s = 0.97$, $\sigma_8 = 0.80$, $T_0 = 2.7255\,\mathrm{K}$. Note that we apply our method to the pre-reconstruction data and thus only calculate the monopole of the clustering. The estimate of multi-poles requires the reconstructed data which will be presented in future works.

2 DATA AND METHOD

In this section, we will first describe the data and mock catalogues used in our study and then review the essential formalism to extract the signals of BAO from the observed galaxies positions.

2.1 Data and Mocks

We use the public data catalogues from SDSS-III BOSS DR12 (Alam et al. 2015), which consist of LOWZ and CMASS samples that occupy $3.7\mathrm{Gpc}^3$ and $10.8\mathrm{Gpc}^3$, respectively. The LOWZ sample has totally $361,762$ galaxies covering the redshift range $0.15 < z < 0.43$, of which $248,237$ galaxies are from the North Galactic Cap and $113,525$ galaxies are from the South Galactic Cap. The CMASS sample has total $777\,202$ galaxies covering the redshift range $0.43 < z < 0.70$, of which $568\,776$ galaxies are from the North Galactic Cap and $208,426$ galaxies are from South Galactic Cap. The total number of data galaxies we used for our analysis is $1,138,964$.

The random galaxy catalogues corresponding to the DR12 data galaxy catalogues are generated by the MKSAMPLE code as descried in Reid et al. (2016) to reproduce the geometry, redshift distribution, and completeness of the survey. In these random samples, the redshift distribution is the same as that in the real data. In Sec.3 we will discuss two different kind of redshift assignments of random catalogues.

Since we only have one Universe to observe, simulations of the observed galaxy clustering are crucial for determining the errors of the measurements. The mock catalogues were generated for this purpose to calculate the covariance matrix for the measured 2PCF. The QPM mock catalogues (White et al. 2014) are generated using rapid, low-resolution particle mesh simulations, which mimic the observed data on both angular selection function and redshift distribution as well as the noise level. The fiducial cosmology is the same as we used in this paper. We use 1000 QPM mock catalogues for each sample (LOWZ or CMASS). The mock catalogues can be used not only to estimate the errors, but also to test the reliability of certain methods. We will test our method of generating random sample with the smooth redshift distribution with the QPM mock catalogues in subsection 3.3.

2.2 Correlation Function

The two-point correlation function (2PCF) estimates the galaxy clustering by counting the excess of data-data galaxy pairs relative to those of random-random galaxy pairs. Here we use the Landy and Szalay estimator (Landy & Szalay 1993),

$$\xi(r) = \frac{DD(r) - 2DR(r) + RR(r)}{RR(r)}, \quad (1)$$

where $DD(r)$, $DR(r)$ and $RR(r)$ are the normalized number count of data-data, data-random and random-random galaxy pairs, respectively. This estimator could minimize the variance to the Poisson level and account for the survey geometry.

Each galaxy carries several weights to correct for possible observational effects, therefore the number counts for galaxy pairs should be weighted as following,

$$GG(r_\alpha) = \sum_{G_i,G_j} w(G_i)w(G_j)\Theta_{r_\alpha}(d_{ij}),\ G = D, R; \quad (2)$$

$$\Theta_{r_\alpha}(d_{ij}) = \begin{cases} 1, & r_\alpha \leqslant d_{ij} < r_\alpha + \Delta r; \\ 0, & \text{otherwise}, \end{cases} \quad (3)$$

where d_{ij} is the separation between pairwise galaxies G_i and G_j, and $G_{i,j}$ stands for galaxy i, j. The specific choices of the weights for the data galaxy $w(D)$ and random galaxy $w(R)$ will be presented in section 3.

2.3 Fitting Template

The fitting model (Xu et al. 2013; Anderson et al. 2013, 2014a) for the monopole moment of 2PCF is parameterized as

$$\xi_{\rm model}(r) = B_0^2\xi_{\rm theory}(\alpha r) + A_0 + \frac{A_1}{r} + \frac{A_2}{r^2}, \quad (4)$$

where the first nuisance parameter B_0 is a normalization factor, and the other three nuisance parameters $A_{0,1,2}$ are introduced to account for any broad-band derivations from the theoretical 2PCF $\xi_{\rm theory}(r)$. The dilation parameter α is defined by

$$\alpha = \frac{D_V(z)/r_{\rm d}}{(D_V(z)/r_{\rm d})_{\rm fiducial}}. \quad (5)$$

The BAO peak position shifts towards smaller (larger) scale if $\alpha > 1$ ($\alpha < 1$) with respect to the fiducial cosmology.

The l-th moment of theoretical 2PCF $\xi^{(l)}_{\rm theory}(r)$ is the Fourier transformation

$$\xi^{(l)}_{\rm theory}(r) = i^l \int \frac{k^2{\rm d}k}{2\pi^2} j_l(kr) P^{(l)}_{\rm nonlinear}(k) \quad (6)$$

of the l-th multipole of non-linear power spectrum $P^{(l)}_{\rm nonlinear}(k)$,

$$P^{(l)}_{\rm nonlinear}(k) = \frac{2l+1}{2}\int_{-1}^{1} {\rm d}\mu L_l(\mu) P_{\rm nonlinear}(k,\mu), \quad (7)$$

The anisotropic non-linear power spectrum $P_{\rm nonlinear}(k,\mu)$ (Fisher et al. 1994) is modeled as

$$P_{\rm nonlinear}(k,\mu) = \frac{(1+\beta\mu^2)^2}{(1+k^2\mu^2\Sigma_s^2)^2} P_{\rm dewiggle}(k,\mu), \quad (8)$$

where $(1+\beta\mu^2)^2$ accounts for the Kaiser effect (Kaiser 1987) and $1/(1+k^2\mu^2\Sigma_s^2)^2$ for the Finger-of-God (FoG) effect (Park et al. 1994). $\beta = f/b$ where $f \approx \Omega_{\rm m}(z)^{0.55}$ is the growth rate and b is the galaxy bias with respect to dark matter. The de-wiggled power spectrum (Eisenstein et al. 2007a; Xu et al. 2013; Anderson et al. 2013, 2014a; Vargas-Magaña et al. 2015) models the degradation the BAO feature due to non-linear structure growth,

$$P_{\rm dewiggle}(k,\mu) = [P_{\rm linear}(k) - P_{\rm nowiggle}(k)] \times \exp\left[-\frac{k^2\mu^2\Sigma_\parallel^2 + k^2(1-\mu^2)\Sigma_\perp^2}{2}\right] + P_{\rm nowiggle}(k). \quad (9)$$

where both the linear theory power spectrum $P_{\rm linear}(k)$ (Lewis et al. 2000) and no-wiggle power spectrum $P_{\rm nowiggle}(k)$ (Eisenstein & Hu 1998) are well approximated in details in Eisenstein & Hu (1998).

We only focus on the monopole of 2PCF with the pre-reconstructed samples. The anisotropic fitting of higher moment of 2PCF with reconstructed samples will be reserved for future works. In this study, we set the streaming scale $\Sigma_s = 4h^{-1}$ Mpc, the radial component $\Sigma_\parallel = 10h^{-1}$ Mpc and transverse component $\Sigma_\perp = 6h^{-1}$ Mpc of the standard non-linear Gaussian damping scale $\Sigma^2_{\rm non-linear} = (\Sigma^2_\parallel + \Sigma^2_\perp)/2$ as inferred from Vargas-Magaña et al. (2015). The spatial separations of interest are chosen from $4h^{-1}$ Mpc to $204h^{-1}$ Mpc with binning size of $8h^{-1}$ Mpc. The fitting range is between $30 \sim 180h^{-1}$ Mpc also with binning size of $8h^{-1}$ Mpc as in the SDSS-III BOSS DR12 (Cuesta et al. 2016). Therefore the total number of points to be fitted is 19 and the fitting parameters to be used are $B_0, \alpha, \beta, A_0, A_1, A_2$, leaving 13 degrees of freedom. The initial values and Gaussian priors $[0 \pm 0.4, 1 \pm 0.1, 0.4 \pm 0.2]$ are adopted for $[\log B_0^2, \alpha, \beta]$.

The χ^2 goodness-of-fit indicator is defined by

$$\chi^2 = \sum_{i,j}[\xi_{\rm model}(r_i) - \xi_{\rm data}(r_i)]C^{-1}_{ij}[\xi_{\rm model}(r_j) - \xi_{\rm data}(r_j)], \quad (10)$$

where the covariance matrix is given by

$$C_{ij} = \frac{1}{N_{\rm mock}-1}\sum_{n=1}^{N_{\rm mock}}[\xi_n(r_i) - \bar{\xi}_{\rm mock}(r_i)][\xi_n(r_j) - \bar{\xi}_{\rm mock}(r_j)], \quad (11)$$

Here $\bar{\xi}_{\rm mock}(r_i)$ is the mean value averaging over the corresponding 2PCF from all QPM mock catalogues at separation bin r_i. To have a unbiased estimation of the inverse covariance matrix (Hartlap et al. 2006), one has to multiply the covariance matrix (11) by

$$C_{ij} \to \frac{N_{\rm mock}-1}{N_{\rm mock} - N_{\rm data} - 2} C_{ij}, \quad (12)$$

where the number of mocks is $N_{\rm mock} = 1000$ and the size of data vector is $N_{\rm data} = 19$. One can also marginalize over the other five parameters for the fixed value of α and obtain the probability density function (PDF) as

$$p(\alpha_i) = \exp\left(-\frac{\chi^2(\alpha_i)}{2}\right) \Big/ \int {\rm d}\alpha_i \exp\left(-\frac{\chi^2(\alpha_i)}{2}\right), \quad (13)$$

based on which we can calculate the mean $\langle\alpha\rangle$ and the variance $\sigma^2_\alpha = \langle\alpha^2\rangle - \langle\alpha\rangle^2$.

Table 1. Galaxy sample and random sample with wiggly method and smooth method both for the DR12 data and for the QPM mocks. $N_{\rm g}(z)$ is the observed redshift distribution, $N_{\rm r}$ is redshift distribution generated with wiggle method. $N_{{\rm g},i}$ is the redshift distribution of the i-th mock sample, $N_{\rm s}$ is the observed redshift distribution weighted by $w_{\rm sys}$, N_w is the observed redshift distribution weighted by $w_{\rm sys}$ and $w_{\rm FKP}$ and $N_{{\rm w},i}$ is the redshift distribution of the i-th mock sample weighted by $w_{\rm sys}$ and $w_{\rm FKP}$. Here $w_{\rm sys}$ is the systematic weight accounting for the observational systematic effects, and $w_{\rm FKP}$ is the Feldman-Kaiser-Peacock weight to reduce the Poisson noise.

	Wiggly Method				Smooth Method			
	DR12 Data		QPM Mock		DR12 Data		QPM Mock	
	redshift population	weight for pair-count	redshift population	weight for pair-count	redshift population	weight for pair-count	redshift population	weight for pair-count
galaxy sample	$N_{\rm g}(z)$	$w_{\rm sys}\cdot w_{\rm FKP}$	$\{N_{{\rm g},i}(z)\}_{i=1}^{1000}$	$w_{\rm sys}\cdot w_{\rm FKP}$	$N_{\rm g}(z)$	$w_{\rm sys}\cdot w_{\rm FKP}$	$\{N_{{\rm g},i}(z)\}_{i=1}^{1000}$	$w_{\rm sys}\cdot w_{\rm FKP}$
random sample	$\frac{N_{\rm r}(z)}{N_{\rm s}(z)}\approx 50$	$w_{\rm FKP}$	$\frac{N_{\rm r}(z)}{N_{{\rm s},i}(z)}\approx 50$	$w_{\rm FKP}$	fitting $N_{\rm w}(z)$	1	$\left\{\begin{array}{c}\text{fitting}\\ N_{{\rm w},i}(z)\end{array}\right\}_{i=1}^{1000}$	1

3 RANDOM CATALOGUES

In this section, we describe the wiggly scheme and smooth scheme of redshift distributions used to generate the random galaxy catalogues, which are summarised in Table 1.

3.1 Wiggly Method

The recent analysis (e.g. Reid et al. 2016) of galaxy clustering utilises the observed redshift distribution of data galaxy catalogues to generate the random galaxy catalogues. This can be mimicked using the following procedure. With redshift bin size $\Delta z = 0.001$, the observed data galaxies redshift distribution for each redshift bin z_α,

$$\begin{aligned} N_{\rm g}(z_\alpha) &= \sum_{D_i}\Theta_{z_\alpha}(z_{D_i}),\\ \Theta_{z_\alpha}(z_{D_i}) &= \left\{\begin{array}{ll} 1, & z_\alpha\leqslant z_{D_i}<z_\alpha+\Delta z;\\ 0, & \text{otherwise,}\end{array}\right. \end{aligned} \tag{14}$$

is a wiggly curve along redshift direction, of which the fluctuations could contain both BAO signals and spurious fluctuations that caused by observational systematic effects and Poisson noises.

The observational systematic effects can be corrected by assigning each data galaxy with a systematic weight (Ross et al. 2016) given by

$$w_{\rm sys}(D_i) = w_{{\rm star},i}w_{{\rm see},i}(w_{{\rm cp},i}+w_{{\rm noz},i}-1), \tag{15}$$

where $w_{{\rm star},i}w_{{\rm see},i}$ are the total angular systematic weights which contribute little to those wiggles of redshift distribution $N_{\rm g}(z)$. The weights $w_{{\rm cp},i}$ that correct for close pairs (fibre collisions) and the weights $w_{{\rm noz},i}$ that correct for redshift failures have little impact on the measured clustering. Therefore the redshift distribution $N_{\rm s}(z)$ corrected by these systematic weights,

$$N_{\rm s}(z_\alpha) = \sum_{D_i} w_{\rm sys}(D_i)\Theta_{z_\alpha}(z_{D_i}), \tag{16}$$

The wiggly method thus generates random catalogues with redshift distribution

$$N_{\rm r}(z)\sim N_{\rm s}(z). \tag{17}$$

Note that the total number of random galaxies is usually larger than the total number of data galaxies, $N_{\rm r}(z) = 50\times N_{\rm s}(z)$, for example in SDSS-III BOSS DR12 (Reid et al. 2016).

The theoretical Poisson noises can also be corrected during pair-counting by assigning each galaxy of pairs the Feldman-Kaiser-Peacock (FKP) weight (Feldman et al. 1994) given by

$$w_{{\rm FKP},i} = \frac{1}{1+n(z_i)P_0}, \tag{18}$$

where $n(z_i)$ is the measured number *density* at redshift z_i with linear interpolation over bins $\Delta = 0.005$ and $P_0 = 20000h^{-3}\,{\rm Mpc}^3$ is the observed power spectrum at $k\approx 0.15h\,{\rm Mpc}^{-1}$. The wiggly method assigns total weights to each galaxy of pairs in different way depending on its type,

$$\begin{aligned} GG(r_\alpha) &= \sum_{G_i,G_j} w(G_i)w(G_j)\Theta_{r_\alpha}(d_{ij});\\ w(D_i) &= w_{{\rm sys},i}\cdot w_{{\rm FKP},i};\\ w(R_i) &= w_{{\rm FKP},i}, \end{aligned} \tag{19}$$

where pairwise galaxies GG can be DD, RR and DR type.

The wiggly method also applies to each QPM mock catalogue labeled by i from 1 to 1000, with their mock random catalogue having the same redshift distribution (17) as the systematically weighted redshift distribution of the mock galaxy catalogue,

$$N_{{\rm r},i}(z)\sim N_{{\rm s},i}(z). \tag{20}$$

The weights assignments for QPM mock galaxy/random catalogues during pair-counting are the same (19) as we do for the DR12 data galaxy/random catalogues.

3.2 Smooth Method

Besides systematic effects and Poisson noises, the observed reshift distribution also could contains fluctuations caused by real structures. A true random catalogue should remove all the spurious fluctuations and only retain a smooth shape of redshift distribution. This motivate us to propose the following smooth method.

When assigning redshifts to the random catalogues, all weights should be taken into account. The observed redshift distribution of data galaxy catalogues, after weighted by both systematic weights and FKP weights,

$$N_{\rm w}(z_\alpha) = \sum_{D_i} w_{\rm sys}(D_i)w_{\rm FKP}(D_i)\Theta_{z_\alpha}(z_{D_i}), \tag{21}$$

gives rise to a less wiggly redshift distribution $N_{\rm w}(z)$, which can be fitted with some smooth functions $N_{\rm f}(z)$. Here we adopt the Moffat function,

$$N_f(z) = \frac{a_0}{\left(\left(\frac{z-a_1}{a_2}\right)^2 + 1\right)^{a_3}} + a_4 + a_5 z. \tag{22}$$

We find this fitting function works better than the one usually adopted in the literature (Ross et al. 2012; Reid et al. 2016). Therefore the smooth method generates random catalogues with redshift distribution,

$$N_{\rm r}(z) \sim N_{\rm f}(z), \tag{23}$$

and assigns weight for each galaxy of galaxy pairs by

$$\begin{aligned} GG(r_\alpha) &= \sum_{G_i, G_j} w(G_i) w(G_j) \Theta_{r_\alpha}(d_{ij}); \\ w(D_i) &= w_{{\rm sys},i} \cdot w_{{\rm FKP},i}; \\ w(R_i) &= 1 \end{aligned} \tag{24}$$

during pair-counting.

The same strategies also apply to each QPM mock catalogue, where its random sample is generated with redshift distribution given by

$$N_{{\rm r},i} \sim N_{{\rm f},i}(z), \tag{25}$$

The weights assignments for QPM mock galaxy/random catalogues for pair-counting are the same (24) as what we do for the DR12 data galaxy/random catalogues.

As a comparison, we present various redshift distributions in Fig.1 for SDSS-III BOSS DR12 data catalogues. As we can see, the random catalogues generated by wiggly method in line with the redshift distribution from the systematically weighted redshift distribution, while the smooth method eliminates the wiggles that are caused by structures.

3.3 Tests on Mock Samples

Before applying to the DR12 data catalogues, we test our smooth method against the wiggly method on QPM mock catalogues. We first select one particular mock which has a rather large scatter in $N_g(z)$ and can thus reflects more clearly the difference caused by different random samples. Three random samples are generated with the wiggly reshift distribution $N_{\rm s}(z)$, the smooth redshift distribution $N_{\rm f}(z)$ and an underlying true redshift distribution respectively. Here the true redshift distribution is assumed to be the averaged value of systematically weighted redshift distribution over 1000 QPM mock galaxy samples,

$$\overline{N}_{\rm s}(z) = \frac{1}{N_{\rm mock}} \sum_{i=1}^{N_{\rm mock}} N_{{\rm s},i}(z). \tag{26}$$

The weight assignment during pair-counting for the random catalogue generated by (26) is as same as the wiggly method (19). As shown in the bottom panels of Fig.2, the measurements of the 2PCF at BAO scale are closer to the true one with our smooth method than the results with the wiggly method. The dilation parameters along with their 1σ errors given by wiggly method, smooth method and true redshift distribution are 0.9906 ± 0.0371, 0.9930 ± 0.0314, 1.0021 ± 0.0339 respectively for LOWZ sample, and 0.9830 ± 0.0178, 0.9736 ± 0.0163, 0.9685 ± 0.0169 respectively for CMASS sample. The volume-average distance $D_V(z) r_{\rm d}^{\rm fid}/r_{\rm d}$ are 1224 ± 46, 1227 ± 39, 1238 ± 42 respectively for LOWZ sample, and 1975 ± 36, 1957 ± 33, 1946 ± 34 respectively for CMASS sample. It shows that both the dilation parameter and the volume-average distance is close to the true one with the smooth method. The 1σ errors are also reduced when adopting the smooth method.

We further apply this procedure to the 1000 mock samples to investigate whether our smooth method can also boost the BAO signals and reduce the error of dilation parameter in general.

Fitting results for the 1000 mocks are shown in Fig.3 with thin curves. Averaged fits are shown with thick curves. As we can see, there is a gentle lift of BAO signals with the smooth method compared to the wiggly method. As in Cuesta et al. (2016) we can use this 1000 mock samples to study the distribution of the dilation parameter in order to quantify the difference of these two methods. We found that, with wiggly method, the dilation parameter α and its 1σ error σ_α and the standard derivation S_α are 1.00134, 0.03430, 0.03215 for LOWZ sample and 1.00055, 0.02081, 0.01980 for CMASS sample respectively. With smooth method, the dilation parameter α and its 1σ error σ_α and the standard derivation S_α are 1.00352, 0.03301, 0.03040 for LOWZ sample and 1.00052, 0.01949, 0.01840 for CMASS sample respectively. It is obvious that, with our smooth method, the 1σ error σ_α and the standard derivation S_α are reduced both for the LOWZ and the CMASS mock samples, though the magnitude is only of order $\mathcal{O}(0.001)$, similar to other systematic effects (Vargas-Magaña et al. 2016).

4 RESULTS

In this section, we apply our smooth method to the SDSS-III BOSS DR12 data catalogues for both LOWZ and CMASS samples and compare the results to those with wiggly method. The results are presented in Fig.4 and Tab.2.

In the top panels of Fig.4, the 2PCF are shown for LOWZ sample and CMASS sample with wiggly method and smooth method. Red curves are the best-fitting results and error bars are obtained from the square root of the diagonal elements of the covariance matrix, which is obtained from the QPM mock catalogues. As we can see, there is a gentle lift of BAO signals with our smooth method with respect to the wiggly method. This exactly meets our expectation for the smooth method, where a more randomly populated catalogue along redshift direction necessarily wipe out residual fluctuations of clustering signals inherited from the measured redshift distribution. Therefore a more pronounced BAO signal is obtained with smooth method.

In the bottom panels of Fig.4, we present the likelihood surfaces for a grid of fixed dilation parameter α from isotropically fitting the 2PCF for LOWZ sample (left) and CMASS sample (right) with wiggly method (red) and smooth method (blue) using fitting templates with (solid) and without (dashed) BAO feature. Each likelihood surface has been subtracted with their minimum χ^2 values. The difference in χ^2 between the template with and without BAO feature reflects the significance of detection of BAO. The χ^2 minimum is slightly narrowed down with our smooth

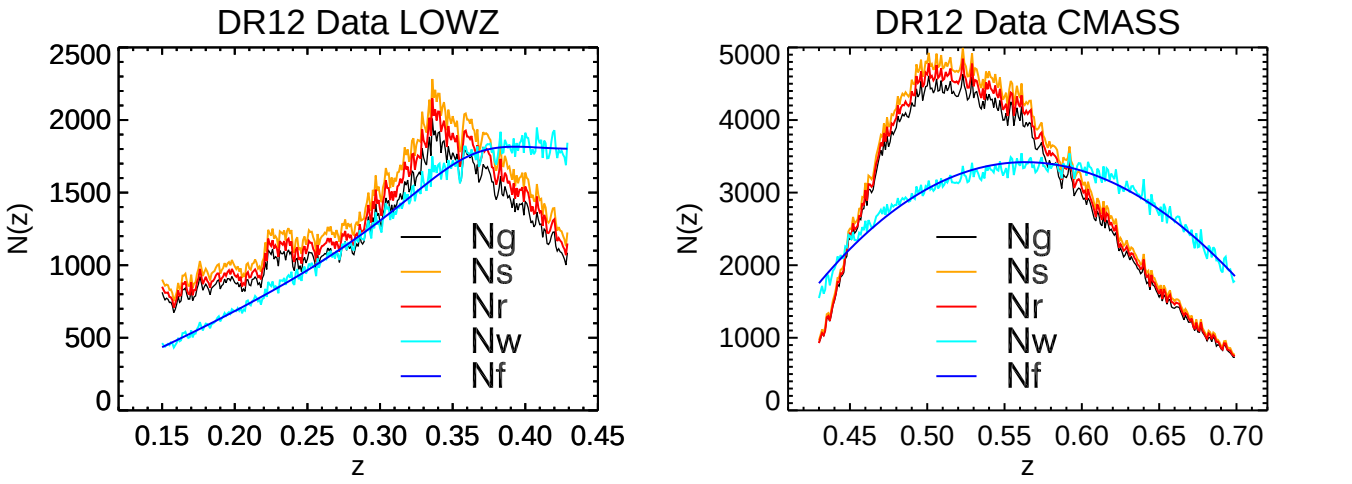

Figure 1. Redshift distributions of the DR12 data catalogs for LOWZ sample (left) and CMASS sample (right). Different samples are presented with different colors as indicated in the each panel. See text and Tab.1 for the definition of each sample. It shows that the smooth method eliminates those wiggles presented in $N_{\rm w}(z)$. All redshift distributions have been scaled properly for clearness.

Table 2. Results for the DR12 data catalogues. In the upper part of the table, the best fit results of dilation parameter α are shown along with their 1σ errors σ_α, which can be used to constrain the volume-average distance to the effective redshifts of LOWZ sample $z = 0.32$ and CMASS sample $z = 0.57$. In the lower part of the table, the mean value of dilation parameter α are shown along with their 1σ errors $\sigma_\alpha = \sqrt{\langle\alpha^2\rangle - \langle\alpha\rangle^2}$. The detection significance is calculated from the square root of difference of χ^2 from the de-wiggled and no-wiggled template at the minimum of χ^2 surface. The upshot of these results is that there is a gentle but uniform improvement on the error of dilation parameter and the detection significance for the DR12 data catalogues.

2PCF $\xi(r)$	$\alpha \pm \sigma_\alpha$	$D_V(z)\frac{r_{\rm d}^{\rm fid}}{r_{\rm d}}$	χ^2/dof
DR12 LOWZ			
wiggly method	1.0175 ± 0.0343	1257 ± 42	6.5/13
smooth method	1.0153 ± 0.0322	1254 ± 40	8.3/13
DR12 CMASS			
wiggly method	1.0148 ± 0.0178	2039 ± 36	10.1/13
smooth method	1.0077 ± 0.0174	2025 ± 35	10.5/13
PDF $p(\alpha)$	$\langle\alpha\rangle$	σ_α	$\sqrt{\Delta\chi^2_{\rm min}}$
DR12 LOWZ			
wiggly method	1.0199	0.0585	2.80σ
smooth method	1.0158	0.0465	3.09σ
DR12 CMASS			
wiggly method	1.0154	0.0173	5.25σ
smooth method	1.0087	0.0168	5.40σ

method compared to the wiggly method, which indicates a minor improvement on the constraint of dilation parameter. The upshot of the bottom panels of Fig.4 is that both the significance of detection of BAO and the constraint on the dilation parameter have been improved gently with our smooth method over the wiggly method.

In Tab.2, we briefly summarize the fitting results of 2PCF for LOWZ sample and CMASS sample. In the upper part of the Tab.2, the best fit results of dilation parameter α are shown along with their 1σ errors σ_α, which can be used to constrain the volume-average distance to the effective redshifts of LOWZ sample $z = 0.32$ and CMASS sample $z = 0.57$. Although the shift of dilation parameter is minor with smooth method and with wiggly method, both LOWZ and CMASS samples have exhibited an uniform reduction on the error of dilation parameter with our smooth method over the wiggly method. In the lower part of the Tab.2, we present the fitting results from probability density function (PDF) of for LOWZ sample and CMASS sample. The mean value of dilation parameter α are shown along with their 1σ errors $\sigma_\alpha = \sqrt{\langle\alpha^2\rangle - \langle\alpha\rangle^2}$ and the detection significance. The significance of detection of BAO has been improved by 0.29σ for LOWZ sample and 0.15σ for CMASS sample. Although the boosted signals and reduced error are necessarily small, it would be appreciated for the future improvements on the measurements of galaxy clustering given the high precise of the measurements of cosmological parameters.

5 CONCLUSIONS

The measurements of galaxy clustering on BAO scale have reached unprecedented precision since the DR11 of BOSS of SDSS-III. Further improvements require more careful understanding of the potential errors. The 2PCF of galaxy clustering measures the number excesses of the data-data galaxy pairs with respect to the random-random galaxy pairs. Therefore a random sample with proper redshift distributions is necessary to recover the BAO signals. In this paper, we propose to use a smooth function which fits the observed galaxy redshift distribution to generate the random galaxy catalogue. It has the advantage to remove the BAO signals along the redshift direction compared with the wiggly method that usually adopted in the literatures, which assignes each random galaxy a redshift by randomly draw-

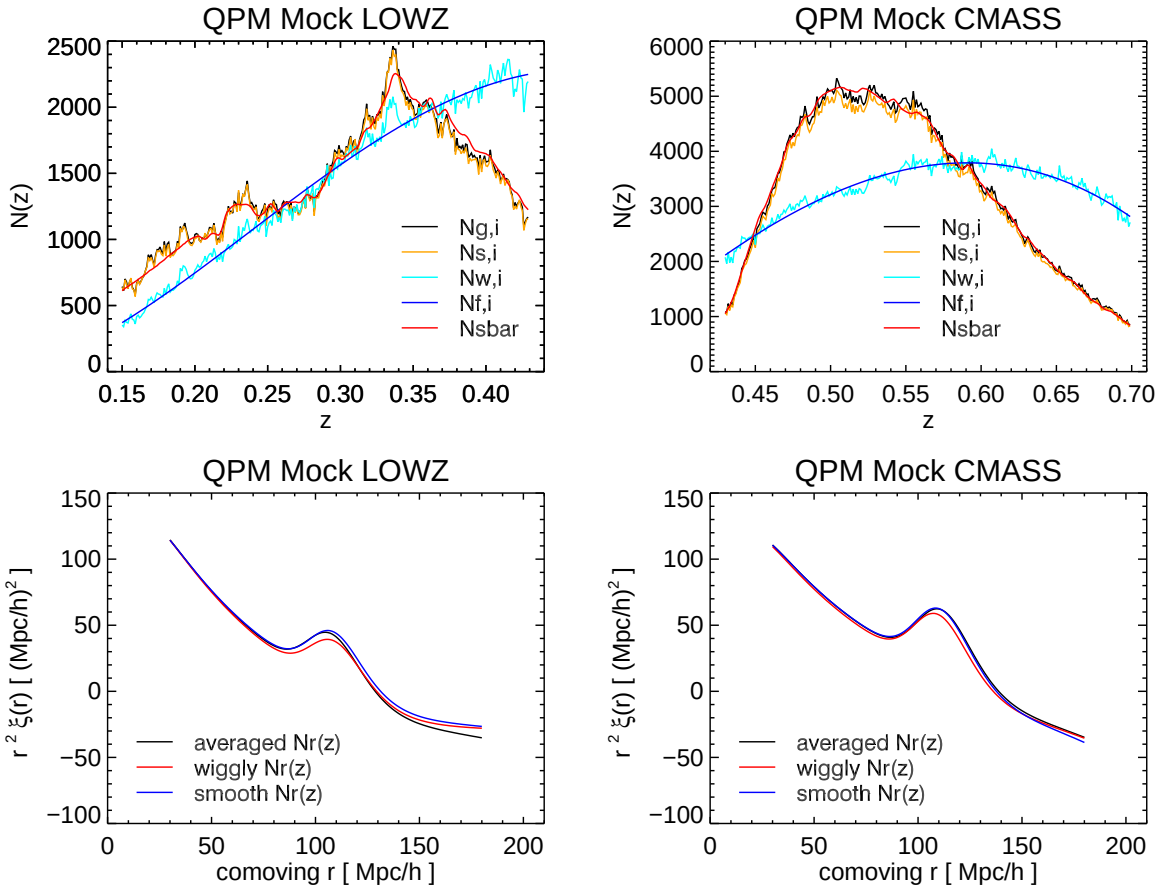

Figure 2. Top panels: redshift distribution for one particular QPM mock catalogue (the i-th one) for both LOWZ (left column) and CMASS (right column) samples. Different colors are for different sample definitions as denoted in the right corner of each panel. The fluctuation of $N_{\mathrm{w},i}$ is rather big to illustrate the effect. Bottom panels: 2PCFs calculated with random samples generated with wiggly method, smooth method and the true redshift distribution are shown with red, blue and black curves, respectively. Results with the smooth method are closer to the true one compared to the wiggly method.

ing a value from the observed redshift distribution, and can thus boost the measured BAO signals. Using the mock data, we demonstrate that the smooth method is capable of improving BAO signals and reducing the errors compared with the wiggly method. When applying to the SDSS DR12 data, we find with the smooth method, we can improve the significance of BAO signals by 0.29 σ and 0.15σ for the LOWZ and CMASS samples, respectively. The rather small improvements is expected, because both LOWZ and CMASS samples cover rather large volume and the sample size is large, which means that the observed redshift distribution suffers little from cosmic variance. For studies which contain smaller samples, for example, the QSO sample, a smooth method could be more helpful in improving the results. Moreover, as discussed in Ross et al. (2012) although the effect of redshift distribution on the monopole of the clustering could be ignored, its effect is large for multi-poles. We will explore this effect with post-reconstruction data in future works.

ACKNOWLEDGEMENTS

We want to thank Antonio J. Cuesta and Benjamin Alan Weaver of SDSS-III BOSS DR12 for the help on BAO fitting. We also want to thank Yuting Wang, Gong-Bo Zhao and Bin Hu for helpful discussions. SJW want to thank Shuangpeng Sun, Shihong Liao, Junyi Jia, Zhen Jiang, Chunxiang Wang for the help on IDL coding and Wei-Ming Dai, Li-Wei Ji for the help on Fortran coding during this work. SJW also want to thank the hospitality of Misao Sasaki when the work was finished during the visit at the Center for Gravitational Physics of Yukawa Institute for Theoretical Physics of Kyoto University. We acknowledge the use of the cluster PANGU and NOVA of NAOC. Qi Guo is supported by NSFC grant (No. 11573033, 11622325), the Strategic Priority Research Program "The Emergence of Cosmological Structure" of the Chinese Academy of Sciences (No.XDB09000000) and the "Recruitment Program of Global Youth Experts" of China, the NAOC grant (Y434011V01). Rong-Gen Cai is supported in part by the Strategic Priority Research Pro-

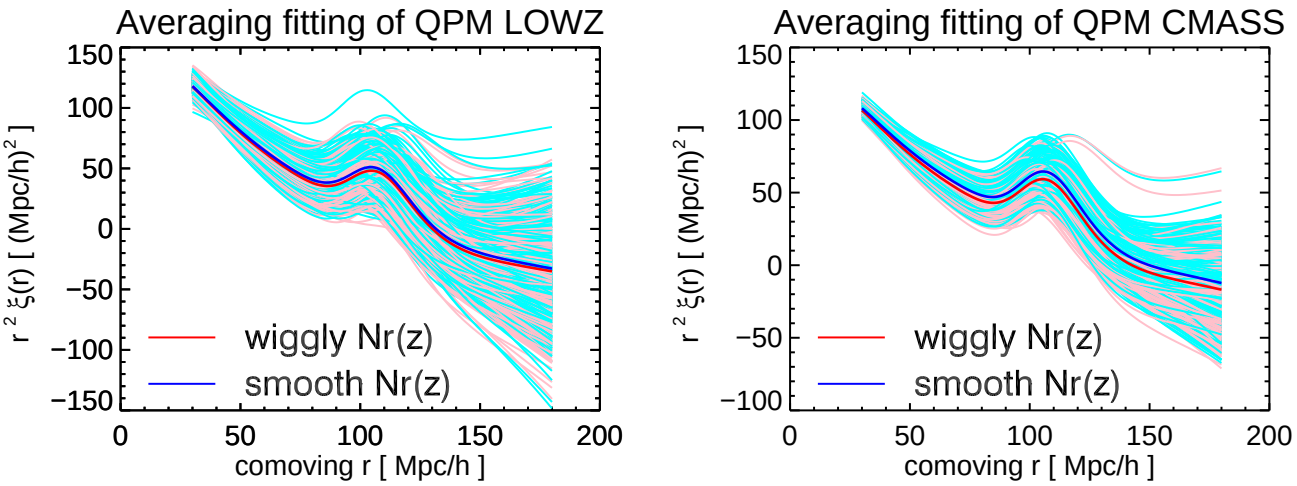

Figure 3. The fitting results of 2PCF of all the 1000 LOWZ (left) and CMASS (right) mock samples with wiggly method (red) and smooth method (blue). Each thin curve represents for one mock results. The averaged 2PCFs are presented with thick curves. The 2PCF at BAO scale is slightly lifted with the smooth method over the wiggly method both for LOWZ and CMASS mock samples.

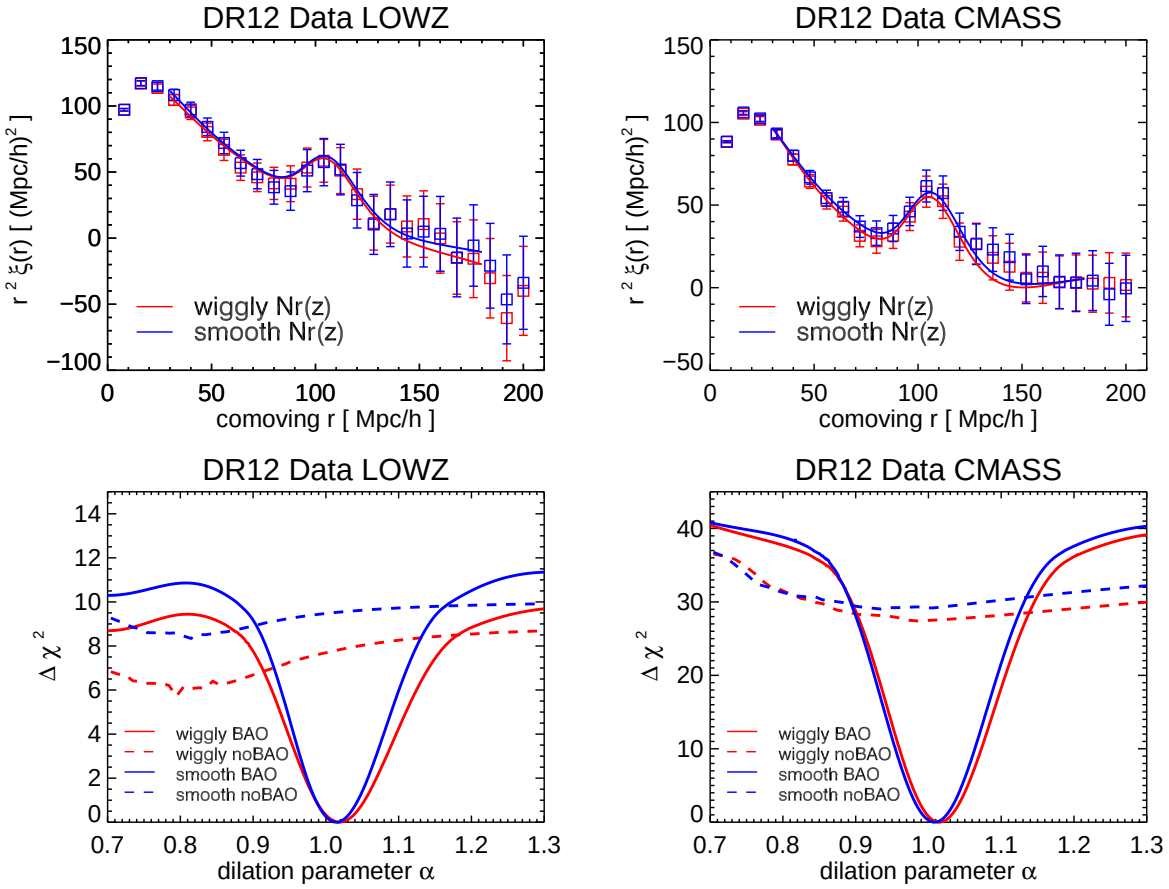

Figure 4. The 2PCF (top) and χ^2 surface (bottom) for DR12 data catalogues are shown for LOWZ sample (left) and CMASS sample (right) with wiggly method (red) and smooth method (blue). In the top panels, there is a gentle lift of BAO signals with the smooth method over the wiggly method. In the bottom panels, it shows a minor improvement of detection significance for the BAO signals.

gram of the Chinese Academy of Science (CAS), Grant No.XDB09000000 and by a key project of CAS, Grant No.QYZDJ-SSW-SYS006 and by the National Natural Science Foundation of China under Grants No.11375247 and No.11435006.

REFERENCES

Alam S., et al., 2015, Astrophys. J. Suppl., 219, 12
Alam S., et al., 2016, Submitted to: Mon. Not. Roy. Astron. Soc.
Alcock C., Paczynski B., 1979, Nature, 281, 358
Anderson L., et al., 2013, Mon. Not. Roy. Astron. Soc., 427, 3435
Anderson L., et al., 2014a, Mon. Not. Roy. Astron. Soc., 439, 83
Anderson L., et al., 2014b, Mon. Not. Roy. Astron. Soc., 441, 24
Beutler F., et al., 2011, Mon. Not. Roy. Astron. Soc., 416, 3017
Blake C., et al., 2011a, Mon. Not. Roy. Astron. Soc., 418, 1707
Blake C., et al., 2011b, Mon. Not. Roy. Astron. Soc., 418, 1725
Chuang C.-H., Wang Y., 2012, Mon. Not. Roy. Astron. Soc., 426, 226
Chuang C.-H., Wang Y., 2013, Mon. Not. Roy. Astron. Soc., 431, 2634
Cole S., 2011, Mon. Not. Roy. Astron. Soc., 416, 739
Cole S., et al., 2005, Mon. Not. Roy. Astron. Soc., 362, 505
Cuesta A. J., et al., 2016, Mon. Not. Roy. Astron. Soc., 457, 1770
Eisenstein D. J., Hu W., 1998, Astrophys. J., 496, 605
Eisenstein D. J., et al., 2005, Astrophys. J., 633, 560
Eisenstein D. J., Seo H.-j., White M. J., 2007a, Astrophys. J., 664, 660
Eisenstein D. J., Seo H.-j., Sirko E., Spergel D., 2007b, Astrophys. J., 664, 675
Feldman H. A., Kaiser N., Peacock J. A., 1994, Astrophys. J., 426, 23
Fisher K. B., Scharf C. A., Lahav O., 1994, Mon. Not. Roy. Astron. Soc., 266, 219
Gaztanaga E., Cabre A., Hui L., 2009, Mon. Not. Roy. Astron. Soc., 399, 1663
Hartlap J., Simon P., Schneider P., 2006, Astron. Astrophys.
Kaiser N., 1987, Mon. Not. Roy. Astron. Soc., 227, 1
Kazin E. A., Sanchez A. G., Blanton M. R., 2012, Mon. Not. Roy. Astron. Soc., 419, 3223
Kazin E. A., et al., 2013, Mon. Not. Roy. Astron. Soc., 435, 64
Landy S. D., Szalay A. S., 1993, Astrophys. J., 412, 64
Lewis A., Challinor A., Lasenby A., 2000, Astrophys. J., 538, 473
Okumura T., Matsubara T., Eisenstein D. J., Kayo I., Hikage C., Szalay A. S., Schneider D. P., 2008, Astrophys. J., 676, 889
Padmanabhan N., White M. J., 2008, Phys. Rev., D77, 123540
Padmanabhan N., Xu X., Eisenstein D. J., Scalzo R., Cuesta A. J., Mehta K. T., Kazin E., 2012, Mon. Not. Roy. Astron. Soc., 427, 2132
Park C., Vogeley M. S., Geller M. J., Huchra J. P., 1994, Astrophys. J., 431, 569
Reid B., et al., 2016, Mon. Not. Roy. Astron. Soc., 455, 1553
Ross A. J., et al., 2012, Mon. Not. Roy. Astron. Soc., 424, 564
Ross A. J., et al., 2016, Mon. Not. Roy. Astron. Soc.
Taruya A., Saito S., Nishimichi T., 2011, Phys. Rev., D83, 103527
Vargas-Magaña M., Ho S., Fromenteau S., Cuesta A. J., 2015
Vargas-Magaña M., et al., 2016
White M., Tinker J. L., McBride C. K., 2014, Mon. Not. Roy. Astron. Soc., 437, 2594
Xu X., Cuesta A. J., Padmanabhan N., Eisenstein D. J., McBride C. K., 2013, Mon. Not. Roy. Astron. Soc., 431, 2834

This paper has been typeset from a TEX/ LATEX file prepared by the author.